HISTIDINE AND CYSTEINE CAN ENHANCE THE METABOLIC REACTION RATES IN THE TCA CYCLE AND SOME AUTOTROPHIC PROCESSES: GENETIC CODE WORLD

Mikio Shimizu*
Institute of Space and Astronautical Science
Yoshinodai, Sagamihara, Kanagawa Prefecture, 229-8510
*Prof. Emeritus
Present mailing address: 1738-6, Kohgasaka, Machida, Tokyo, 194-0014;
Tel: 042-723-7584; E-mail address: mshimizu55@ybb.ne.jp

(Abstract)

It was found that cysteine or its ester can enhance various reaction rates in the TCA cycle such as aconitase, isocitrate dehydrogenase, succinate dehydrogenase, and fumarase and that histidine or its ester can enhance those such as succinate CoA synthetase and citrate synthase. Histidine or its ester can also enhance the reaction rates for carbonyl aspartate dehydrogenase, 2-keto-3-deoxy octonate aldolase, and acetoacetate decarboxylase. These findings for the origins of metabolism as well as those for the origins of the genetic code and the central metabolic pathway in our recent publications [2-4] suggest that life would have started from a system of amino acids and anticodonic tri-ribonucleotides. Some possible routes to the contemporary biosystem from this "genetic code world" were discussed.

Keywords: amino acid enzyme, anticodon ribozyme, TCA cycle, autotrophe, genetic code world

1. Introduction

The central metabolic pathway of biosystem is consisted of two major processes: (1) the energy acquiring pathway such as Embden-Meyerhoff pathway (or non- phosphorylated Entner-Doudorff pathway in thermophiles) and (2) the TCA cycle [1]: The former cleavages glucose (C_6 sugar) to pyruvate (C_3 sugar) and then to form acetyl CoA. The latter starts from the reaction between acetyl CoA and oxalacetate to form citrate, which is converted to various organic acids successively, and finally to oxalacetate, the first substrate of the cycle. The cycle produces many starting substrates converting to amino acids, nucleotides, and lipids later.

The results in my previous letter [2] showed that histidine acts as pyruvate carboxylase (ligase) to form oxalacetate from pyruvate and carbonate with ATP , as oxalacetate decarboxylase (lyase) to cleave oxalacetate to pyruvate and CO_2, and as glucose-6-phosphate isomerase (isomerase) weakly but specifically. GpUpG, the anticodon of histidine, had also a similar enzymatic activity stronger by one order of magnitude than that of histidine, which showed a specific relationship between an amino acid and an anticodon, namely the stereochemical theory of the genetic code.

I have also shown in a separate letter [3] that not only histidine but other single amino acids such as cysteine, glutamic acid (or aspartic acid), lysine, and tyrosine (and their cognate anticodons, too) can act as the specific catalysts of various metabolic reactions including transferase and oxido-reductase in addition to the three classes of enzymes discussed

in the previous letter [2]. Furthermore, it will be studied in another paper [4] that two single amino acid, histidine or cysteine, can convert glucose to pyruvate and then to acetyl CoA and ATP (via non-phosphorylated Entner-Doudorff pathway) catalytically.

In this report, I shall attempt to check that all reactions in the TCA cycle can also be enhanced by histidine and cysteine. Furthermore, some other important metabolic reactions for autotroph of the system will be investigated. Photometry will be used to find the catalytic capacity of these amino acids, measuring the initial velocities of the reactions. Confirmation of the formation of the reaction products will be attempted using cold thin layer chromatography (TLC) and high performance liquid chromatography (HPLC).

2. Materials and Methods

2.1. Materials

All biochemicals were from Sigma. Some amino acids exhibit rather low solubility. We found in preliminary experiments that the esters of amino acid, which were blocked at their carboxyl groups and are much more soluble than the amino acids themselves, could act as the substitutes of corresponding amino acids, while N-acetyl amino acids , which are blocked at their amino group, usually lacked rate-enhancing activity. We employed the esters when high concentrations of amino acids were required to detect weak interactions. For leucine, isoleucine, methionine, phenylalanine, tyrosine, and tryptophan, we used their methyl or ethyl esters, or t-butyl ester for glutamine. Their rate-enhancing behaviors were the same as those of the corresponding amino acids at an equimolar concentration. Some of the amino acids such as lysine, arginine, aspartic acid, and glutamic acid are of salt form. The counter ions of the Tris and acetate buffers are hydrochloride and sodium, respectively.

2.2. Enzymatic Assays

We examined all twenty proteinaceous amino acids to determine their rate-enhancing activities in the metabolic reactions one after another. At first, the specific reactivity was measured using the sensitive spectrophotometry. The substrates were solved in the buffer solution and mixed successively, adding the amino acid- buffer solution at last. Absorbance of the above mixture solution poured in the cell of the Beckmann DU 65 spectrophotometer was measured periodically. The experiments were performed at room temperature ($25\ ^0$C). In the following photometric assays, 100 µl of the reaction mixture, whose final concentrations were specified in the figure captions of each reaction were used.

The above spectroscopic assays were performed as described in the standard data handbooks [5, 6]. Each assay will be described in the figure caption, as well as the adopted reactant concentrations.

In the following reactions, the concentrations of amino acids are much higher than those of the reaction substrates. Consequently, almost all the substrates combine with the amino acid catalyst at first, in contrast to the usual catalytic reaction where enzymes are almost fully occupied with the substrates quickly before the final catalytic reaction proceeds.

In the cold TLC, the two dye were used : (1) silver nitrate with a back colour of brown (1 M silver nitrate aqueous solution 50% and 1 N NaOH solution 50%) for figures 2(b), 5(b), 6(b), and 7(b) and (2) 3-5-dinitrosalitylic acid with a back colour of yellow (0.5% 3-5-dinitrosalitylic acid in 4N ammonia aqueous solution) for figures 3(b). The reaction products were usually developed in the buffer of 70 % n-propanol -30 % 2 M ammonia aqueous solution, except the hexokinase case, spotting 0.2-1 μl of the reaction mixture on the cellulose plate. The R_f's of the spots were determined using authentic samples, which were indicated by arrows in each figure. The cold TLC has two factors, Rf's and colour, and is an adequate method to observe the formation of the reaction products such as citrate, isocitrate, and malate which have no absorption in visible and ultraviolet range and are difficult to detect by the HPLC method.

The confirmation was also done using HPLC, where the reaction mixture was applied into a RPC 5 column (Nishio Tech. Co.). The used wavelength is 260nm. The elution buffer started from pH 7.8 Tris 1 mM buffer with a linear gradient of 20 % of 0.1 M sodium perchlorate solution in 24 minutes. The positions of the peaks of various compounds were determined using the authentic samples.

Disposable tips and tubes were sterilized at 190 ^{0}C and 1.5 atm. for 10 minutes.

3. Results
3.1. TCA cycle

Here, we study amino acid catalysts in the TCA cycle, one after another, in the presence of various coenzymes such as NAD^+, FAD^+, and CoA. Byproducts in this cycle could be used for the production of amino acids as well as nucleotides. Figure 1 summarize the scheme of the studied reactions [1].

Aconitase, isocitrate dehydrogenase (abbreviated as DH later), alpha ketoglutarate DH-type activities of cysteine: These three reactions can be enhanced by cysteine or its ester (Cys or CE). Figure 2(a) and Figure 3(a) illustrate the increase of NADH absorption at 340 nm for aconitase and isocitrate DH, respectively. Nineteen other amino acids (19 aa), or the reference (which replaces the amino acid buffer solution by the buffer solution) did not result in the decrease of absorption. Figure2(b) depicts a TLC plate showing the cis-aconitate $COOHCH_2C(COOH)CH(OH)COOH$ spot (left) before the reaction and the formation of an isocitrate $COOHCH_2CH(COOH)CH(OH)COOH$ spot near the origin of elution (right) after the reaction. Figure 3(b) illustrates the appearance of an

alpha-ketoglutarate $COOHCH_2CH_2COCOOH$ spot after the reaction (right), while an isocitrate spot is seen on the left plate before the reaction. The reaction scheme of alpha-ketoglutarate DH is similar to that of pyruvate DH, which will be
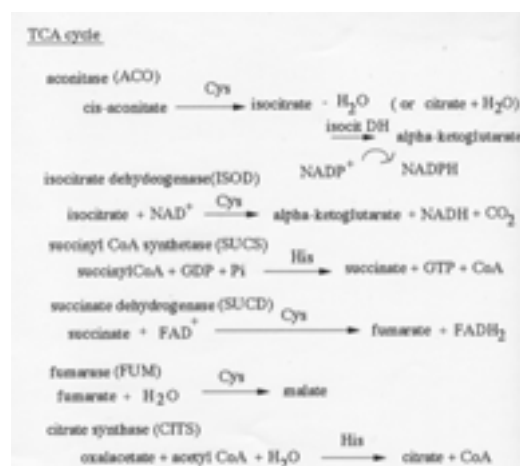

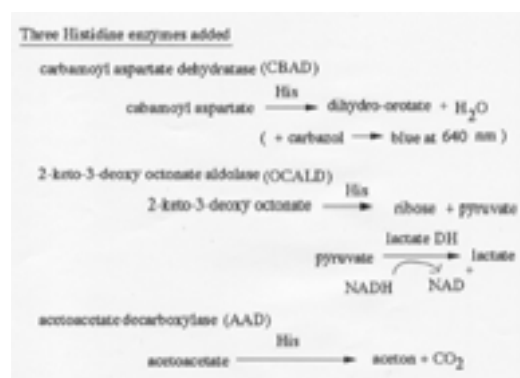Figure 1. Reaction scheme for the studied metabolic reactions.
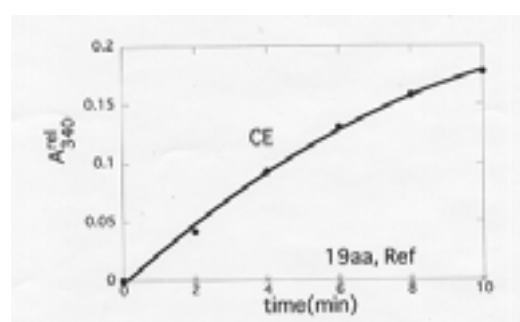

Figure 1. Continued.

Figure 2(a). (ACO) Time sequence of aconitase activity of cysteine ethyl ester (CE) using the coupled enzymatic method with isocitrate dehydrogenase by use of the absorbance at 340 nm of NADPH . A^{rel}_{340} means the relative absorbance at 340 nm to the absorbance at t = 0. Final concentration: pH7.8 Tris buffer 100mM, cis-aconitate 1 mM, $NADP^+$ 0.3 mM, *Porcine Heart* isocitrate dehydrogenase 3 units and cysteine ethyl ester or 19 other amino acids, 10 mM. Nineteen other amino acids and the reference showed very low activity due to the spontaneous reaction.
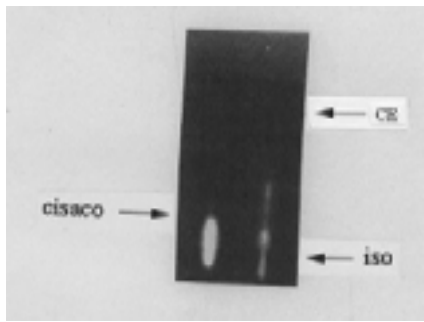
Figure 2(b). (ACO) A cellulose TLC plate showing the disappearance of cis-aconitate (cisaco) and appearance of isocitrate (iso) after the reaction time of 1 day (right) in the presence of cysteine ethyl ester (CE). In the left figure, the spots for the reaction mixture at zero time were shown. This is the same below. The top and bottom of the figure indicate the end and start of elution. The positions of authentic samples were indicated by arrows: CE for cysteine ethyl ester, cisaco for cis-aconitate, and iso for isocitrate. Final concentration: pH 7.5 Tris buffer 300 mM, cis-aconitate 50 mM, and cysteine ethyl ester 200 mM.

Figure 3(a). (ISOD) Time sequence of isocitrate DH activity of cysteine ethyl ester (CE) observing the absorbance of NADH at 340 nm. Final concentration: pH 7.8 Tris buffer 100 mM, isocitrate 100 mM, NAD$^+$ 100 mM, cysteine ethyl ester and 19 other amino acids 100 mM.
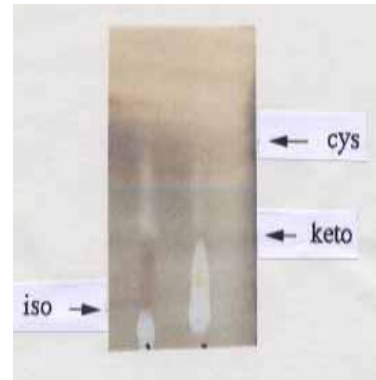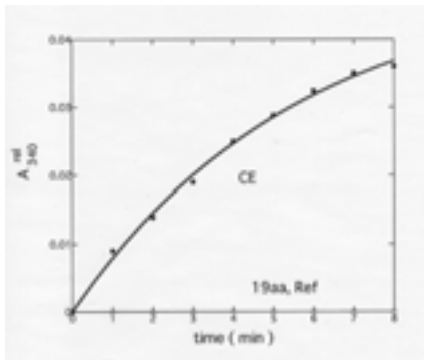

Figure 3(b). (ISOD) A TLC plate showing the disappearance of isocitrate (iso) and appearance of alpha-ketoglutarate (keto) after the reaction time of 1 day in the presence of cysteine. Final concentration: Tris pH 7.8 buffer 100mM, isocitrate 50 mM, NAD$^+$ 20mM, cysteine 100mM.
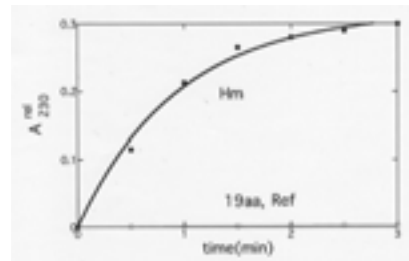

Figure 4(a). (SUCS) Time sequence of succinyl CoA synthetase activity of histidine methyl ester (Hm) observing the absorbance of succinyl CoA at 230 nm. Final concentration: pH 7.8 phosphate buffer 50 mM, succinate 20 mM, CoA 10 µM, GTP 10 µM , and histidine methyl ester or 19 other amino acids 5 mM.
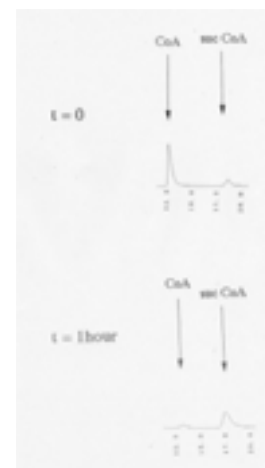

Figreu 4(b). (SUCS) HPLC diagrams of the reaction mixture after 0 and 1 hour for the succinyl CoA synthase activity of histidine methyl ester (Hm). Arrows show the positions of the molecules determined by eluting authentic samples. The formation of succinyl CoA and the decrease of CoA were confirmed. Final concentration: pH 7.8 Tris buffer 100 mM, succinate 50 mM, GTP 20 mM, CoA 50 mM, histidine methyl ester 100 mM.

discussed in another paper [4] in details. Consequently I shall not attempt to study this process here.

Succinyl CoA synthetase- type activity of histidine: For this activity, I checked the reverse reaction to form succinyl CoA from succinate, CoA and GTP. Figure 4(a) depicts the time sequence of succinyl CoA COOHCH$_2$CH$_2$COSCoA absorption at 230 nm in the presence of histidine methyl ester (Hm). Nineteen other amino acids and the reference showed no change. Figure 4(b) illustrates a HPLC diagram showing the formation of succinyl CoA from CoA and succinate by the succinyl CoA synthetase-type activity of histidine methyl ester (Hm) after 1 hour. PiP and succinate COOH CH$_2$CH$_2$COOH have no absorption at 260nm.

Succinate DH, fumarase, and malate DH-type activities of cysteine: All these reactions are correlated with cysteine or its ester. Malate DH will

be discussed in another paper. Figure 5(a) and 6(a) show the decrease of FAD^+ absorption at 448 nm, and that of fumarase $COOHCH=CHCOOH$ absorption at 280 nm, respectively.

Figure 5 (b) illustrates the disappearance of a succinate tenuous spot and the formation of a fumarate spot near the origin of elution after the reaction by a TLC experiment. Rf of the fumarate spot is almost zero, loosing the information from this quantity. However, the grey white color of the spot is completely similar to the fumarate spot in the Figure 6(b) for fumarate, which endorses the formation of this molecule in the succinate DH reaction. Figure 6(b) is the TLC plate for the fumarase reaction. The presence of a malate spot appeared after the reaction in addition of a fumarate spot near the origin of elution. Malate DH will be discussed in another letter [3].

Citrate synthase-type activity of histidine: Acetyl CoA $CH_3COSCoA$ and oxalacetate $COOHCH_2COCOOH$ would form citrate $COOHCOCOH(COOH)CH_2COOH$ and CoA (HSCoA) in the presence of histidine. Figure 7(a) depicts the time sequence of the decrease of oxalacetate absorption at 290 nm catalyzed by histidine methyl ester. Nineteen other amino acids (19 aa) showed no activity. Imidazole alone[4] did

not result in the decrease of absorption. Figure 7(b) depicts the result of a TLC experiment: the formation of a citrate spot after the reaction (right) might be confirmed. In the figure 7(c) for a HPLC experiment, the formation of CoA and the decrease of acetyl CoA and oxalacetate after 3 hours was demonstrated.
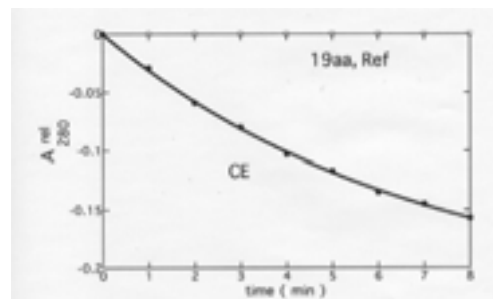
Figure 6(a). (FUM) Time sequence of fumarase activity of cysteine ethyl ester (CE) observing the absorbance of fumarate at 280 nm.
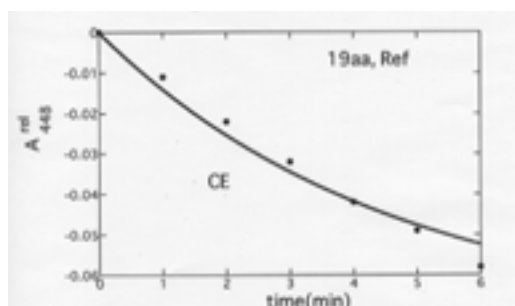Final concentration: pH 7.8 Tris buffer 100 mM, fumarate 5 mM, cysteine ethyl ester or other amino acids 100 mM.

Figure 5(a). (SUCD) Time sequence of succinate dehydrogenase activity of cysteine ethyl ester (CE) observing the absorbance of FAD^+ at 448 nm. Final concentration: pH 7.8 Tris buffer 100 mM, succinate 10mM, FAD^+ 10 mM, cysteine ethyl ester or 19 other amino acids 100 mM.

Figure 6(b). (FUM) A TLC plate showing the appearance of malate (mal) after the reaction time of 1 day in the presence of cysteine. Final concentration: pH 7.8 Tris buffer 300 mM, fumarate (fum) 50 mM, cysteine 100 mM.
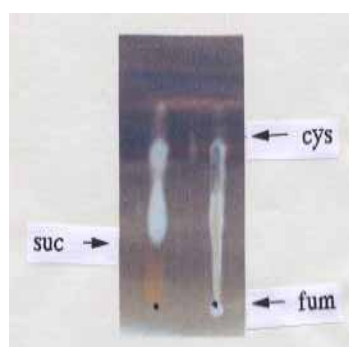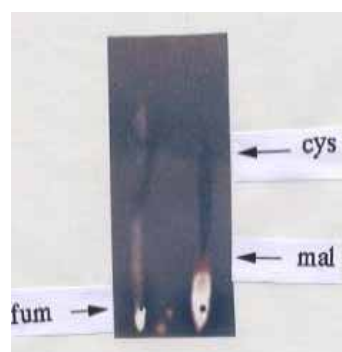

Figure 5(b). (SUCD) A TLC plate showing the disappearance of succinate (suc) and appearance of fumarate (fum) near origin of development after the reaction time of 1 day in the presence of cysteine. Final concentration: pH 7.8 Tris buffer 100 mM, succinate 50 mM, FAD^+ 50 mM, cysteine 100 mM.
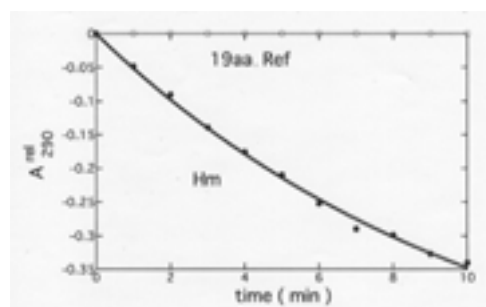

Figure 7(a). (CITS) Time sequences of citrate synthase activity of histidine methyl ester (Hm) determined by the absorbance of oxalacetate at 290 nm at 25^0C. Final concentration: pH7.9 Tris buffer 100 mM, oxalacetate 10 mM, acetyl CoA 10 mM, and histidine methyl ester or 19 other amino acids 100 mM.

3.2. Three histidine enzymes

Here I shall discuss three important histidine enzymes in addition to amino acid enzymes in the TCA cycle. Carbamoyl aspartate dehydration is a typical reaction to form nucleic acid ring from a linear molecule. Together with alanine amino transformation reaction by histidine in another letter [3] , which is also a typical reaction in amino acid formation, the autotrophic character of genetic world may be expected. Cleavage of 2-keto-3deoxy gluconic acid is the most important process in the central pathway of thermophiles (non-phosphorylated Entner-Doudorff pathway), as shown in a coming paper [4]. However, this molecule was not obtained commercially. Consequently, the experiment of cleavage of 2-keto-3-deoxy octonic acid here is a good direct example to certify the possibility above.

Nucleic acid ring formation (Carbamoyl aspartate dehydratase): Figure 8(a) illustrates the increase of dihydroorotate absorption at 240 nm in the presence of histidine. The HPLC diagrams in Figure 8 (b) of the reaction mixture depicts the formation of dihydroorotonate $-NHCONHCH(COOH)$ CH_2CO-, where – means a ring connection, peak from the carbamoyl aspartate
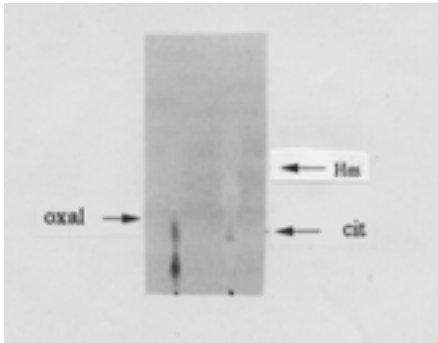

Figure 7(b). (CITS) TLC spots on a cellulose plate for the citrate synthase activity of histidine methyl ester: (left) the oxalacetate spot was clearly seen by eluting the reference solution at zero time. Right lane is that for the reaction mixture after the reaction time of 1 day. Formation of citrate and decrease of oxalacetate were demonstrated. : oxal for oxalacetate, Hm for histidine methyl ester, cit for citrate. The final concentration: pH 7.9 Tris buffer 100mM, oxalacetate 50 mM, acetyl CoA 10 mM, histidine methyl ester 100 mM.
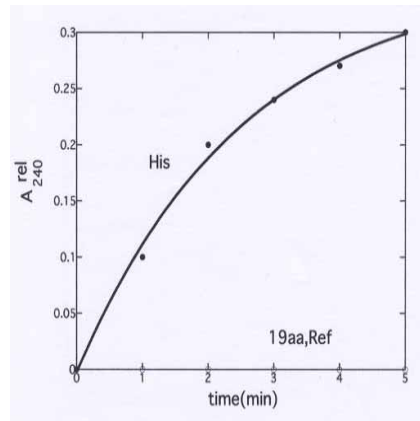

Figure 8(a). (CBAD) Time sequence of carbamoyl aspartate activity of histidine observing the absorbance of dihydroorotate at 240 nm. Final concentration: pH 7.8 Tris buffer 100 mM, carbamoyl aspartate 25mM, and histidine 50 mM.
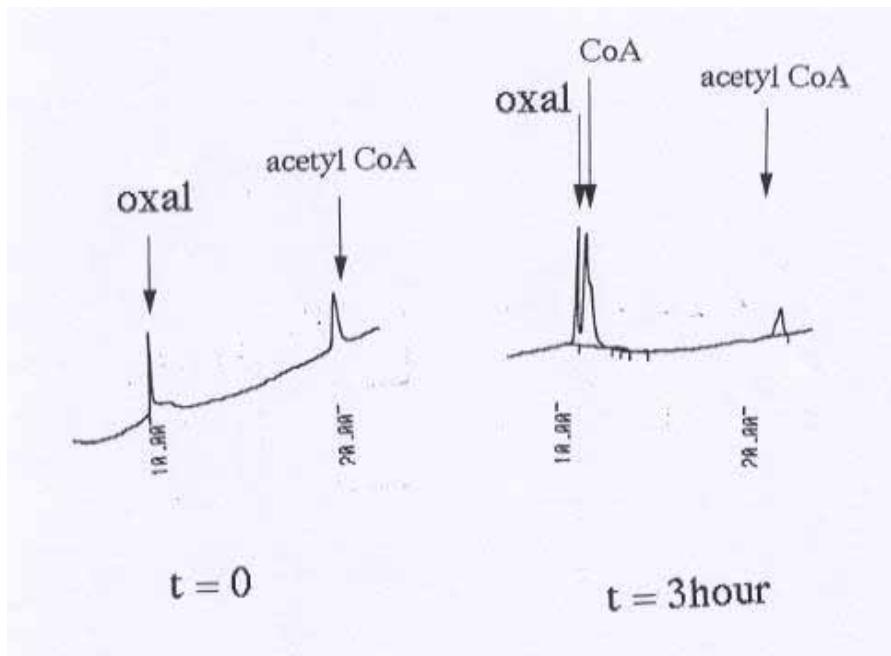

Figure 7(c). (CITS) HPLC diagrams of the reaction mixture after 0 and 3 hours for the citrate synthase activity of histidine. Formation of CoA after 3 hours was confirmed. The ratio of the integrated absorbance of oxalacetate to that of acetyl CoA at t=0 is 1/2, while the ratio of oxalacetate to (CoA + acetyl CoA) is1/3.6. Consequently the amount of oxalacetate was decreased during the time. Final concentration: pH 7.8 Tris buffer 100 mM, oxalacetate 25 mM, acetyl CoA 25 mM, and histidine 50 mM.
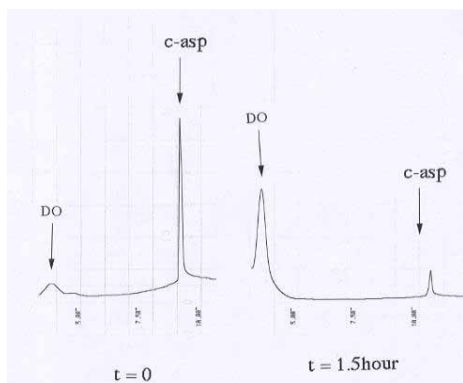
Figure 8(b). (CBAD) HPLC diagrams of the reaction mixture after 0 and 1.5 hour for the carbamoyl aspartate dehydratase activity of histidine. The formation of dihydroorotate was confirmed by observing the appearance of its peak and decrease of the carbamoyl aspartate. DO for dihydroorotate and c-asp for carbamoyl aspartate. Final concentration: the same as in Fig. 8(a).
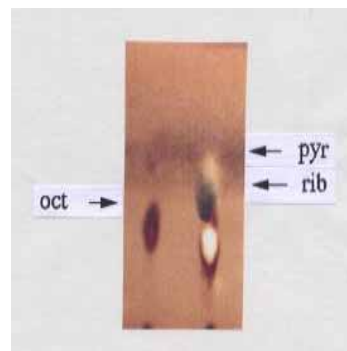

Figure 9(b). (OCALD). A TLC plate showing the appearance of pyruvate (pyr) and ribose (rib) after the reaction time of 1 day in the presence of histidine (right).

In the left figure, the reference solution at t=0 was shown, since the white histidine spot hides the octonate spot. Final concentration: pH 5.9 acetate buffer 100 mM, 2-keto-3-deoxy octonate 50 mM, histidine 100 mM.
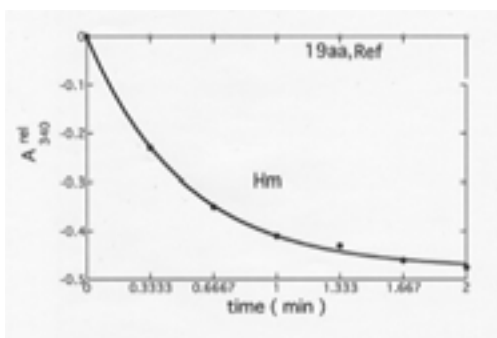

Figure 9(a) (OCALD). Time sequence of 2-keto-3-deoxy octonate aldolase activity of histidine methyl ester (Hm) using the coupled enzymatic method in the presence of lactic dehydrogenase to reduce the produced pyruvate observing the absorbance of NADH at 340 nm. Final concentration: pH 5.9 acetate buffer 100 mM, 2-keto-3-deoxyoctate 100 mM, NADH 0.12 mM, *Rabbit Muscle* lactate dehydrogenase 10 units, and histidine methyl ester or 19 other amino acids 100 mM.
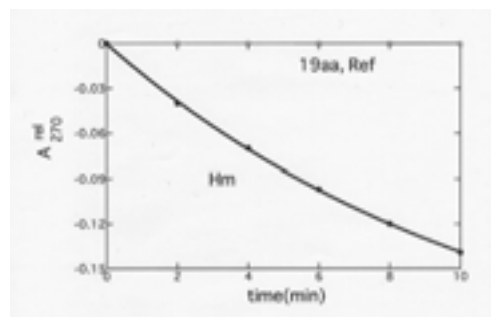

Figure 10(a). (AAD) Time sequence of acetoacetate decarboxylase activity of histidine methyl ester (Hm) observing the absorbance of acetoacetate at 270 nm. Final concentration: pH 5.9 phosphate buffer 200 mM, acetoacetate 10 mM, histidine methyl ester 100 mM.

$NH_2CONHCH(COOH) CH_2COOH$ leaving H_2O.

2-keto-3-deoxy octonate aldolase-type activity of histidine: Figure 9(a) shows, by the addition of histidine ethyl ester, the decrease of NADH absorption at 340 nm reacted with the produced pyruvate from 2-keto-3-deoxy octonate $CHOCOCH_2(CHOH)_4CH_2OH$ in the presence of lactate DH. Nineteen other amino acids, the reference had no effect. Figure 9(b) is the TLC plate showing the appearance of pyruvate and ribose $CHO(CHOH)_4CH_2OH$ from 2-keto-3-deoxy octonate in the presence of histidine.

Acetoacetate decarboxylase-type activity of histidine: Figure 10 (a) illustrates the decrease of acetoacetate by measuring the absorption at 270 nm in the presence of histidine, while 19 other amino acids and the reference result in no change of absorption. Figure 10(b) depicts the formation of aceton peak from acetoacetate. It also shows that tyrosine had no effect in this reaction.

4. Discussions on histidine and cysteine enzymes

For the majority of the metabolic reactions studied above, one amino acid enhances one reaction rate specifically. Cysteine was found to mainly participate in the oxidoreductive reactions and histidine was found to participate in the acid-base reactions. These two amino acids are known to exhibit activity in the electron and group transfer reactions, respectively: their side chains contain thiol and imidazole, respectively, which are the most electron-mobile group best for catalysis among those of the twenty amino acids [1]. However, imidazole itself showed no enzymatic activity. The amino group of histidine is needed. Formalization of various rate-enhancing mechanisms of each reaction was not attempted here. However, it is instructive to discuss the difference among amino group (in the peptidyl moiety of amino acids) catalyst, a residue (of amino acids) catalyst, and an amino acid catalyst. I shall show in another paper [4] that extraction of water from gluconic acid to form 2-keto-3-deoxy gluconic acid was catalyzed by various amino acids. In these

cases, the amino group in the peptidyl moiety of the amino acids is responsible for the reactions. It is also known that para-nitrophenyl acetic acid is hydrolyzed by histidine. The imidazole group of histidine works as a catalyst [1]. In contrast, the amino acid catalyst uses both the amino group (base) and the residue (acid) for catalysis (for instance, of acid-base type).

One interesting result is that the amino acid rate-enhancers for aconitase and fumarase are cysteine, not histidine which most frequently appeared in the cases of lyase (dehydratase in these cases). It is known that aconitase contains sulphur in its catalytic center [1] similarly to cysteine. Another histidine dehydratase, 2-keto-3-deoxy *octonate*
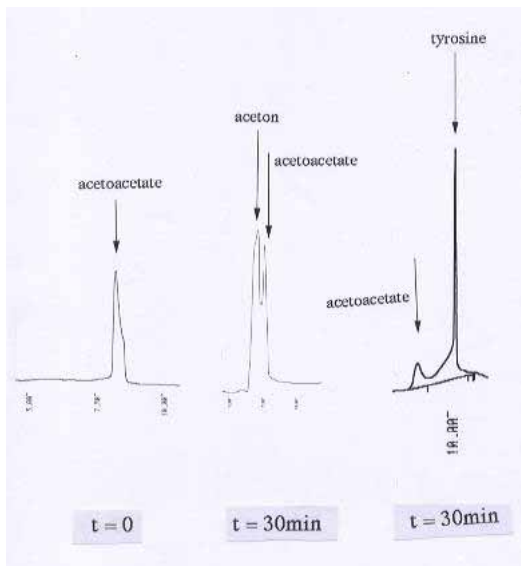
Figure 10(b). (AAD) HPLC diagrams of the above reaction mixture after 0 and 30 min for the acetoacetate decarboxylase activity of histidine. The formation of aceton was observed for histidine, but not for tyrosine. (Furthermore, addition of Tris buffer 10 μl to the solid mixture of acetoacetate 1 mg and histidine 1 mg caused degassing of CO_2, another good evidence for the histidine catalyst; (data not shown.).

aldolase, is essential for cleaving glucose to pyruvate and glyceraldehyde in the central metabolic pathway in the ancient bacteria and archaea. NADH formed in the TCA cycle might have been oxidized by the nitrate fermentation [7] using cysteine (corresponding to nitrate oxidoreductase) and nitrate instead of oxygen and the electron transfer system in the contemporary ATPase- membrane system. In the contemporary biosystem, succinate DH is located in the membrane and uses FAD^+ instead of NAD^+ as an oxidant, and produced $FADH_2$ is oxidized by the electron transfer system. Primitively, FAD^+ may oxidize succinate to fumarate directly.

5. Origin of Primitive protein Synthetic System

We have already shown that some amino acids have specific affinity ($1 M^{-1}$) to their cognate anticodonic nucleotides in the genetic code table [8-10]. It was also found [11] that the anticodons in the contemporary tRNAs could have stronger specific affinity ($200 M^{-1}$) to their cognate amino acids.

In the contemporary biosystem, catalysts are proteins which are formed by the protein synthetic system containing various complex processes including amino acids, tRNAs (adaptors), aminoacyl-tRNA synthetases, ribosomes and so on (Figure11(c)). It is essentially a catalyst increasing (= protein synthetic) system using RNA. Since amino acids could possess weak catalytic activities for some prebiotic reactions, the above anticodon-cognate amino acid association might be regarded as the oldest protein synthetic system, although it contained no adaptors yet (Figure 11(b)). Anticodons were replicable and the "anticodon world" could be regarded as the smallest genetic system (in a sense, it forms a smallest RNA world). The anticodons would be the most primitive "genes"、in the meaning that they attract the catalytic amino acids into the primitive cell (or increase the numbers of the smallest "enzymes" there).

For further evolution to elongate the amino acid to a dipeptide and beyond, we need some
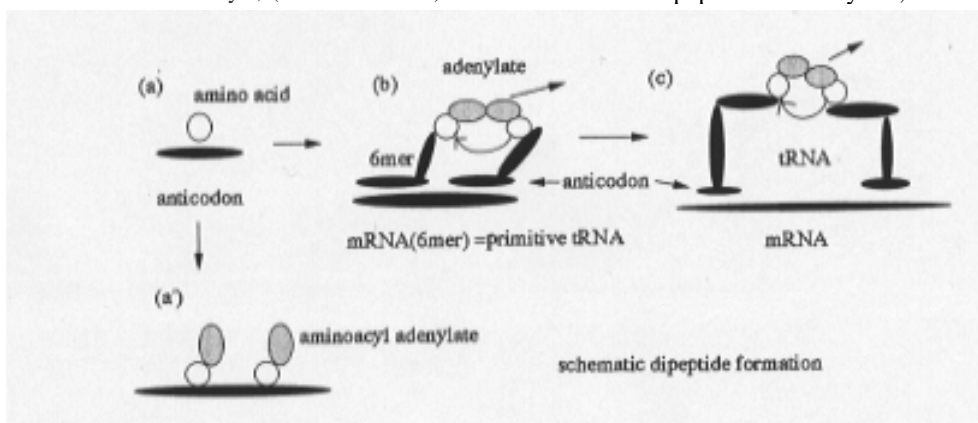
Figure 11. Evolution of dipeptide formation mechanism in the primitive and Contemporary protein synthetic system. (a) affinity between an amino acid and its cognate anticodon is the start of the protein synthetic system. (a') Formation of a dipeptide from two aminoacyl adenylates on 6mer RNA are impossible due to a long distance between the two. (b) a 6mer RNA (mRNA) with two aminoacyl adenylate on another tRNA can make a dipeptide using their long tails. The primitive tRNA is also a primitive gene. (c) contemporary system to form a dipeptide drawn quite schematically, neglecting the ribosome and other apparatus. Of course, an anticodon on mRNA sits next to another anticodon.

adaptors - very short tRNAs as discussed by Crick [12]. Since the distance between two amino acid on a 6mer RNA is too great from each other to make a bond using some energy-supplying molecule (Figure 11(a')), Crick assumed the presence of an adaptor with anticodonic trinucleotides at its 5' end and a tail having an aminoacylated nucleotide at its 3' end (Figure 11(b)). The shortest primitive tRNA of 25 mers with an anticodon at its 5'end and a stem plus the discriminator and CCA trinucleotides at its 3'end was shown to be aminoacylated using aminoacyladenylates and a varylaspartate as the catalyst [13]. The number of the 7 base pairs in the stem could be reduced to 2 (Shimizu, unpublished result). Hopefully, the final goal of this type of approach may be to find a system of 6 mer tRNAs (as a template for the dipeptide, so it could be the primitive gene) and dipeptide catalysts for aminoacylate formation and elongation (Figure 11(b)) . Figure 11 illustrates the above discussion.

6. Relationships of amino acid catalyst to the dipeptide catalysts

I have demonstrated that some dipeptides could function as catalysts in various biochemical reactions: as already discussed, valylaspatate (or varylglutamate) behaved as an aminoacyl transferase[13]. In this relationship, I found that glutamic acid has transferase activity in this paper. Similarly, histidine frequently appeared in the dipeptide catalysts, such as alanylhistidine [14], serylhistidine and glutamylhistidine[15]. The catalytic activity of amino acids had more increased in the dipeptide catalysts. More precise specificity to substrates and higher activity of biocatalysts would have sometimes been sophisticated by the increase in the numbers of amino acids in the catalysts (peptides or proteins) through biochemical evolution.

7. Three concentration mechanisms of amino acids

Amino acid and anticodon rate-enhancers are all weak. Consequently, there should be some concentration mechanisms to increase the concentrations of these compounds in the primitive oceans, if these compounds were correlated with the generation of the life there. Three mechanisms for concentrations in a primitive cell on the primordial earth could be considered:

(1) *Evaporation by heat*: About 3.9 billion years ago, the earth began to cool due to the cease of the infall of planetesimals but locally was still very hot. This was a unique time for generation of life on this planet. From carbon isotope data, photosynthesis would have worked at this time[16]. The concentration of the amino acids in a pool at the seashore near volcanoes would have reached a high level.

(2) *large fluctuation*.: Concentration of amino acids in one of the primitive cells might have increased to 10-100 mM level by *large fluctuation* (see the random drift in Kimura's neutral theory [17] for the evolution of species at a molecular level). Dyson also stressed the importance of rapider random drift against slow selection [18]. It is noteworthy that this discussion could apply to the generation of life in the hydrothermal vents at the bottom of oceans, where employment of the concentration mechanism by evaporation would be difficult.

(3) *Specific association*: If some anticodonic RNAs (about 1.5 nm size) were contained in the primitive cell, the RNA might have formed a complex with an amino acid (about 0.5 nm size) entering the cell from outside. This complex, which have a much larger size than a single amino acid, would have remained in the cell for a longer time than an amino acid would, contributing to an increase in the amino acid concentration.

8. Conclusion

Amino acid-metabolites interactions in the case of the TCA cycle are studied using ultraviolet-visible spectroscopy. These are confirmed by cold thin layer chromatography and high performance liquid chromatography.

The anticodon-codon relationship is the trunk of the concept for inheritance. (In contrast, there is no specific relationship between amino acids. Metabolite-metabolite relationships are mere organic chemistry.) The determination of the DNA structure with a simple symmetry resulted in an intuitive molecular understanding of inheritance. On the other hand, metabolism has no simple symmetry in it and contains so many reactions. The information here and that on the central pathway in another paper [4] may be useful for understanding of primitive metabolism at the small molecular level.

In the genetic code world, the amino acid world and anticodon world are coupled inseparably, supporting both inheritance and metabolism [3]. The anticodon world is the minimal RNA world. The usual RNA polymer (~100mers) world suggested by SELEX faced a great difficulty recently by the finding of high primitive ocean temperature (~80 ^{o}C) due to a good correlation between two mutually independent O (from sea water) and Si (from outside silica) isotope data for old cherts [3,19]. It is noteworthy that amino acids and anticodon could be formed at high temperature such as that of hydrothermal vent.

References

1. Voet, D. and Voet, J. D. Biochemistry, second edition, John Wiley and Sons Inc., New York, 1995.
2. Shimizu, M. Histidine and its Anticodon GpUpG are Similar Metabolic Reaction Rate Enhancers: Molecular Origin of the Genetic Code, J. Phys. Soc. Jpn, 73, 323-326 (2004).
3. Shimizu, M. Amino acid and anticodon enhance metabolic reaction rates weakly but specifically: Genetic code world, Jour. Phys. Soc. Jpn, 76, 053801 (2007).
4. Shimizu, M., Yamagihsi A., Kinosita, K. Sida,T.

and Oshima, T. Histidine and Cysteine can produce acetyl CoA and ATP from Gucose via Reaction homologous to Non-phosphorylated Entner-Doudorff Pathway: Prebiotic Origin of Glycolytic Metabolism, submitted to J. Biochem.

5. Biochemical Data Hanbook II. (Tokyo Kagaku Dohjin, Tokyo ,1980)

6. Dowson, R. M. C., Elliot, D. C., Elliot W. H. and Jones, K. M. Data for Biochemical Research, Oxford Press, NewYork, 1986.

7. Egami, F., Ishimoto M. and Seki-Chiba, S. Nitrate fermentation in *Closeridium perfringens* and significance in metabolic functions, pp. 427-430, in Noda, H. Ed., Origin of Life, Center for Academic, Publications, Japan, Tokyo, 1977.

8. Shimizu, M. Specific interactions of dinucleoside monophosphates with their cognate amino acids, J. Phys. Soc. Jpn , 56, 43-45 (1987).

9. Shimizu, M. A fast atom bombardment study on the interaction of anticodonic nucleotides and their cognate amino acid, Jour. Phys. Soc. Jpn., 56, 893-896 (1987).

10. Shimizu, M. A proton magnetic resonance study on the structure of UpU-lysine complex in relation to the origin of the genetic code, J. Phys. Soc. Jpn., 57, 54-56 (1988).

11. Watanabe, K. and Miura, K. Specific interaction between tRNA and its cognate amino acid as detected by circular dichroism and fluorescence spectroscopy, Biochem. Biophys. Res. Comm., 129, 679-683 (1985).

12. Crick, F. H. C. Discussion in The Structure of Nucleic Acid and their Role in Protein Synthesis, Biochem. Soc. Sympo. No.14, Cambridge Univ. Press, Cambridge, 1957.

13. Shimizu, M. Specific aminoacylation of C4N hairpin RNAs with the cognate aminoacyladenylates in the presence of a dipeptide: Origin of the genetic code, J. Biochem. (Tokyo), 117, 23-29 (1995).

14. Shimizu, M. Detection of the peptidyltransferese activity of a dipeptide, alanylhistidine, in the absence of ribosomes, J. Biochem. 119, 832-834 (1995).

15. Shimizu, M. Violent primitive earth might have harmonized with the origins of life, pp. 431-436, in "Bioastronomical and Biochemical Origins of Life", Proc. IAU colloquium No.161, Edit. Comp., Bologna, Italy, 1997.

16. *Schidlowski, M. The beginning of life: Evidence from geological record, pp. 389-414, in Greenberg, J. M., Mendoza Gomez, C. X. and Pirronello, V. Eds., The Chemistry of Life's Origins, Klewer Academic Press, Netherlands, 1986.

17. Kimura, M. The neutral theory of molecular evolution, Cambridge Press, Cambridge ,1983.

18. Dyson, F. Origins of life, Cambridge Press, Cambridge, 1999.

19. Robert, F. and Chaussidon, M. A paleotemperature curve for the Precambrian oceans based on the silicate isotope in chert, Nature, 443, 969-972 (2006).